

Document downloaded from:

<http://hdl.handle.net/10251/195331>

This paper must be cited as:

Gómez-Gómez, Á.; Brito-De La Fuente, E.; Gallegos, C.; Garcia-Perez, J.; Quiles Chuliá, MD.; Benedito Fort, JJ. (2022). Microbial inactivation by means of ultrasonic assisted supercritical CO₂. Effect on cell ultrastructure. *The Journal of Supercritical Fluids*. 179:1-9. <https://doi.org/10.1016/j.supflu.2021.105407>



The final publication is available at

<https://doi.org/10.1016/j.supflu.2021.105407>

Copyright Elsevier

Additional Information

1 Microbial inactivation by means of ultrasonic assisted supercritical CO₂. Effect on cell
2 ultrastructure

3
4 **Angela Gomez-Gomez^a, Edmundo Brito-de la Fuente^b, Crispulo Gallegos^b, Jose
5 V. Garcia-Perez^a, Amparo Quiles^a and Jose Benedito^a**

6
7 ^a Grupo ASPA, Departamento de Tecnología de Alimentos, Universitat Politècnica de València,
8 Camí de Vera s/n, València, E46022, Spain

9 ^b Fresenius-Kabi Deutschland GmbH, Product and Process Engineering Center,
10 Pharmaceuticals & Device Division, Siemensstraße 27, 61352. Bad Homburg, Germany

11
12 **Abstract**

13
14 The effect of ultrasound (HPU) on the supercritical carbon dioxide (SC-CO₂) inactivation
15 of vegetative bacteria (*Escherichia coli*, *Brevundimonas diminuta*) and a fungal spore
16 (*Aspergillus niger*) at different pressures (100 and 350 bar) and temperatures (35, 50
17 and 60°C) was assessed. The effect of SC-CO₂ + HPU on the microbial cell ultrastructure
18 was also evaluated by microscopy techniques (FESEM and TEM). HPU enhanced the
19 SC-CO₂ inactivation treatments, showing an average increase of 4.8, 3.4 and 1.3 log-
20 cycles of reduction for *E. coli*, *B. diminuta* and *A. niger*, respectively. In general, the
21 higher the pressure and temperature, the higher the inactivation. *A. niger* spores were
22 found to be more resistant than vegetative bacteria. Microscopy analysis revealed
23 significant morphological changes, including damaged cell walls, and major alteration
24 and loss of cytoplasmic content. Therefore, the SC-CO₂ + HPU technology appears to
25 be effective for microbial inactivation purposes despite the complexity of the cell wall.

26
27
28 **Keywords:** supercritical CO₂, high power ultrasound, bacteria, fungal spore,
29 ultrastructure.

31 **1. Introduction**

32 Vegetative bacteria and fungal spores can easily become contaminants of food and
33 pharmaceutical products, leading to product spoilage and causing human disease. In
34 this regard, the assurance of microbiological safety is essential for the industry.
35 Nowadays, thermal treatments are the most common preservation methods in the food
36 and pharmaceutical sectors. In order to prevent heat damage related to thermal
37 treatments and obtain higher quality products, novel non-thermal technologies, applied
38 individually or in combined form, have been investigated and developed during the last
39 few years. Some of these so-called non-thermal technologies are irradiation [1], high
40 power ultrasound [2], pulsed electric fields [3], high hydrostatic pressure [4] and
41 supercritical fluids [5].

42 The supercritical state of carbon dioxide (SC-CO₂) is reached at moderate pressure and
43 temperature (73.8 bar and 31.1°C), avoiding the negative thermal effects of traditional
44 preservation methods. In supercritical conditions, CO₂ presents lower viscosity than
45 when in the liquid state and higher density than when in the gaseous state, making SC-
46 CO₂ an excellent solvent that can contribute to the removal of vital components of
47 microbial cells. In this sense, SC-CO₂ has already proven to be an effective method for
48 the inactivation of some microorganisms, minimally affecting the physicochemical
49 properties of the treated products [6–8]. However, SC-CO₂ treatments often require long
50 processing times and/or high temperatures and pressures to provide the necessary
51 microbial reduction that ensures product safety. As an example, more than 75 min were
52 insufficient to achieve the complete inactivation of *E. coli* in apple juice at 32°C and 100-
53 300 bar [9]. For this reason, it is of great interest to combine the SC-CO₂ treatment with
54 other non-thermal techniques, such as high power ultrasound (HPU), high hydrostatic
55 pressure (HHP) [4], pulsed electric fields (PEF) [10] or the addition of antimicrobial
56 agents, such as hydrogen peroxide [11]. In this regard, the application of HPU to the SC-
57 CO₂ treatments has already been demonstrated to intensify the inactivation of a wide
58 range of vegetative bacteria and yeasts [12,13]. However, the SC-CO₂ + HPU
59 inactivation of filamentous fungal spores has not been explored yet.

60 The most widely accepted inactivation mechanisms of SC-CO₂ are linked to the diffusion
61 and solubilisation of CO₂ into the external media causing a drop in pH that could damage
62 or alter the microbial cell membrane. Thus, CO₂ penetrates into the cells, reducing the
63 internal pH and extracting intracellular vital components which, eventually, can lead to
64 cell death [14]. When HPU is implemented, the heat and mass transfer processes are
65 enhanced due to cavitation effects, which could increase the CO₂ diffusion rate,

66 accelerating the SC-CO₂ inactivation mechanisms. In addition, HPU could damage or
67 crack the cell walls of the microorganisms [12,13]. A better understanding of the
68 inactivation mechanisms exerted by the combination of SC-CO₂ and HPU is important in
69 order to find improved strategies with which to guarantee the safety and stability of the
70 treated products, as well as optimize the process conditions or the equipment. For that
71 purpose, the analysis of the treated microbial cells at cellular level using microscopy
72 techniques constitutes a valuable approach. Several authors observed the ultrastructure
73 of microbial cells after SC-CO₂ inactivation treatments and stated that there was a direct
74 relation between the permeabilization of the cell membrane and the inactivation [15,16].
75 Additionally, Ortuño et al. [17] investigated the effect of the SC-CO₂ + HPU treatment on
76 the intracellular structure of vegetative microorganisms (*E. coli* and *S. cerevisiae*).
77 However, there has been no prior analysis of the cell structural effects linked to the SC-
78 CO₂ + HPU treatment on filamentous fungal spores. Moreover, the analysis of the
79 changes in the external structure of the microbial cells after the SC-CO₂ + HPU treatment
80 is unexplored. Therefore, the objective of this study was to evaluate (i) the intensification
81 of the SC-CO₂ + HPU inactivation of different bacteria (*E. coli* and *B. diminuta*) and a
82 fungal spore (*A. niger*) and (ii) the effect of the inactivation treatment on the external
83 morphology and the intracellular structure of the microbial cells.

84

85 **2. Materials and methods**

86 2.1. Preparation of the bacterial suspensions: *Escherichia coli* and 87 *Brevundimonas diminuta*

88 *E. coli* CECT 101 and *B. diminuta* CECT 313 were obtained from the Spanish Type
89 Culture Collection (CECT, Valencia, Spain). *E. coli* is a facultative anaerobic gram-
90 negative bacteria with a cell size of around 1 × 3 μm [18], highly common in contaminated
91 food and pharmaceutical products. *B. diminuta* is an aerobic gram-negative bacteria,
92 which is used to test the porosity of pharmaceutical grade filters of 0.2 μm because of its
93 small size [19]: typically of around 0.3 x 1.0 μm [20]. A single colony of each bacterium
94 was inoculated in 50 mL of nutrient broth (Scharlab, Barcelona, Spain) and grown
95 overnight (18-24 h) at 37°C for *E. coli* and 30°C for *B. diminuta*, using an incubation
96 chamber (3000957, J.P. Selecta, Spain) and an orbital shaker at 120 rpm (3000974, J.P.
97 Selecta, Spain). 50 μL of the overnight starter culture were transferred to a new growth
98 medium and it was incubated until ensuring the stationary phase was reached, 14 h at
99 37°C for *E. coli* and 36 h at 30°C for *B. diminuta* [21]. After that, 5 mL of the bacterial

100 suspension in the stationary phase were inoculated in 60 mL of deionized water until a
101 concentration of around 10^8 CFU/mL.

102

103 2.2. Preparation of the *Aspergillus niger* spore suspension

104 *A. niger* CECT 2807 was also obtained from the Spanish Type Culture Collection (CECT,
105 Valencia, Spain). *A. niger* is an aerobic spore-forming filamentous fungi, commonly
106 present in the environment and, thus, usually present in contaminated food and
107 pharmaceutical products [22]. *A. niger* was cultured on Potato Dextrose Agar (Scharlab,
108 Barcelona, Spain) at 25°C for 7 days. After that, spores were rubbed with 10 ml of 0.1%
109 (v/v) Tween 80, collected and kept at 4°C until use. Prior to each treatment, 5 mL of the
110 *A. niger* spore suspension were inoculated in 60 mL of deionized water until a
111 concentration of around 10^7 CFU/mL.

112

113 2.3. Ultrasonic assisted supercritical fluid inactivation treatments

114

115 The inactivation treatments with supercritical carbon dioxide (SC-CO₂) were performed
116 in a supercritical fluids lab-scale equipment and batch mode. A high-power ultrasound
117 (HPU) transducer, embedded in the treatment chamber (600 mL of internal volume)
118 through the cap, was used to perform the combined SC-CO₂ + HPU treatments. The
119 ultrasound system consisted mainly of a high power piezoelectric transducer, a
120 sonotrode and a power generation unit. The power supplied was 50 ± 5 W ($I = 250 \pm 10$
121 mA; $U = 220 \pm 5$ V) and the frequency was 30 ± 2 kHz. Electrical parameters were
122 measured with a digital power meter (WT210, Yokogawa Electric Corporation, Tokyo,
123 Japan). This system was explained in detail in a previous study [21].

124 SC-CO₂ and SC-CO₂ + HPU inactivation treatments were carried out on 65 mL of
125 inoculated water at two levels of pressure and temperature for each microorganism. The
126 pressure (pressurization rate of about 70 bar/min) was set at 100 and 350 bar for all the
127 microorganisms, as they are common pressures used in SC-CO₂ microbial inactivation
128 studies [23]. The temperature was set at 35 and 50°C for *E. coli* and *B. diminuta* in order
129 to select a low temperature (35 °C), very close to the critical temperature for CO₂ and a
130 mild, but non-lethal, temperature (50°C) for the vegetative bacteria considered in this
131 study. In this regard, preliminary experiments revealed that no inactivation was found for
132 inoculated *E. coli* and *B. diminuta* in deionized water using a water bath and heating at
133 50°C for 50 min. In the case of *A. niger*, treatments were carried out at 50 and 60°C due

134 to the known greater resistance of fungal spores to SC-CO₂ compared to vegetative
135 bacteria [23]. Samples of around 2 mL were collected (undergoing a sudden
136 depressurization to atmospheric pressure) during the treatments at different times,
137 depending on the process conditions and type of microorganism. All the experiments
138 were carried out in triplicate.

139

140 2.4. Microbiological analyses

141

142 The standard plate count was used to measure the number of surviving microorganisms.
143 Serial dilutions of the treated samples were prepared and 100 µL of the appropriate
144 dilutions were spread on PCA for the bacteria and PDA for *A. niger* (Scharlab, Barcelona,
145 Spain) in triplicate. Plates were incubated at 37°C and 24 h for *E. coli*, 30°C and 48 h for
146 *B. diminuta* and 25°C and 72 h for *A. niger*. The initial microbial population in the sample
147 was determined following the same procedure. Results were expressed as log₁₀ (N/N₀),
148 where N₀ represents the number of cells initially inoculated in the deionized water and N
149 the number of cells after treatment.

150

151 2.5. Modelling

152

153 The non-linear Weibull model following the decimal logarithmic form written by Peleg [24]
154 has been demonstrated to be sufficiently robust for the prediction of microbial inactivation
155 [25], and was used in this study (Eq. (1)).

156

$$157 \log_{10} \frac{N}{N_0} = -b \cdot t^n \quad \text{Eq. (1)}$$

158

159 where N₀ indicates the initial number of microorganisms in the sample (CFU/mL), N is
160 the number of microorganisms in the sample after the treatment time t (CFU/mL), n
161 (dimensionless) is the shape factor and b (min⁻ⁿ) is the rate parameter.

162

163 The constants of the model (b and n) were computed by minimizing the sum of squared
164 differences between the experimental and predicted levels of inactivation using Solver
165 from Microsoft Excel™. The root mean squared error (RMSE, Eq. 2) and the coefficient
166 of determination (R², Eq. 3) were determined to evaluate the goodness of fit.

167

168
$$RMSE = \sqrt{\frac{\sum_{k=1}^z (y_k - y_k^*)^2}{z}}$$
 Eq. (2)

169

170
$$R^2 = 1 - \frac{S_{yx}^2}{S_y^2}$$
 Eq. (3)

171

172 where y and y^* are the experimental and the estimated data, respectively; z is the
173 number of experimental data, and S_{yx} and S_y are the standard deviations of the
174 estimation and the sample deviation, respectively.

175

176 The model can be fitted to both downward concave survival curves ($n > 1$) and upward
177 concave curves ($n < 1$); and the log linear curve is a special case where $n = 1$. As described
178 elsewhere [26], the time required to achieve the complete inactivation (t_x) of every
179 microorganism was calculated from Eq. 1 and from the b and n values of the Weibull
180 model obtained for each condition, where x is the average in log-cycles for the complete
181 inactivation of each microorganism (7.9 log-cycles in the case of *E. coli*, 8.1 log-cycles
182 in that of *B. diminuta* and 6.8 log-cycles for *A. niger*).

183

184 2.6. Statistical analysis

185 In order to evaluate the effect of both the treatment conditions (pressure, temperature
186 and use of HPU) and the type of microorganism on the inactivation, a general linear
187 model (GLM) was performed using Statgraphics Centurion XVI (Statpoint Technologies
188 Inc., Warrenton, VA, USA). Fisher's least significant difference (LSD) was used to
189 discriminate among the means ($p < 0.05$).

190

191 2.7. Electron microscopy observations

192 The microscopy observations of the microbial cells were performed after and before the
193 SC-CO₂ + HPU treatments. The conditions selected were those that achieved the
194 complete microbial inactivation of each microorganism: 50°C, 350 bar and 2 min in the
195 case of *E. coli* and *B. diminuta* and 60°C, 350 bar and 10 min for *A. niger* spores.

196 In order to observe the external morphology of the microbial cells, a field emission
197 scanning electron microscope (FESEM) was used (ZEISS ULTRA 55, Oxford
198 Instruments, Abingdon, UK). To this end, microbial samples were centrifuged at 2600
199 rpm for 5 min and filtered (0.2 µm of pore diameter). Then, samples were placed in the
200 holder, frozen by immersion in liquid nitrogen and transferred to a cryogenic unit

201 (PP3010T, Quorum Technologies, East Sussex, UK) to be sublimated and coated with
202 platinum by sputtering at 5 mA for 20 s. Samples were observed at 1 kV at a working
203 distance of between 3-5 mm.

204 For the observation of the intracellular structure of the microorganisms, transmission
205 electron microscopy (TEM) was used (HT-7800 120 kV, Hitachi High-Technologies,
206 Tokyo, Japan). For this purpose, microbial samples were centrifuged at 2600 rpm for 5
207 min, fixed with 25 g/L glutaraldehyde solution for 24 h at 4 °C and post-fixed with 20 g/L
208 osmium tetroxide solution for 1.5 h. After that, cells were stabilized with agarose solution
209 (3 g/100mL) at 30°C and stored at 4°C for 24 h. The solidified agar with the cells was cut
210 into cubes (3 mm³), which were fixed with 25 g/L glutaraldehyde solution; post-fixed with
211 20 g/L osmium tetroxide solution, dehydrated with 300, 500, 700 and 1000 g/kg ethanol,
212 contrasted with 20 g/L uranyl acetate solution and resin-embedded. The blocks obtained
213 were cut into ultrathin sections (0.1 µm) with Reichert-Jung Ultracut ultramicrotome
214 (Leica Microsystems, Wetzlar, Germany), collected in copper grids and stained with 40
215 g/L lead citrate to be observed at 100 kV.

216

217 **3. Results and discussion**

218 3.1. Analysis of the inactivation kinetics

219 3.1.1. SC-CO₂ microbial inactivation

220 Fig. 1 shows the inactivation kinetics of *E. coli* (A), *B. diminuta* (B) and *A. niger* spores
221 (C) in deionized water for the SC-CO₂ treatments. A high degree of experimental
222 variability was found, as can be observed from the error bars, which could be ascribed
223 to pressure and temperature variations inside the vessel, and to the inherent variability
224 in the microbial growth. Despite the great experimental variability, the Weibull model was
225 satisfactorily fitted to the SC-CO₂ inactivation kinetics, as depicted in Fig. 1. In every
226 case, R² was higher than 0.92 and RMSE was lower than 0.64, as shown in Table 1. For
227 some of the inactivation kinetics, the model was not fitted due to the lack of experimental
228 data.

229 Effect of pressure and temperature

230 Pressure and temperature had a significant ($p < 0.05$) effect on the SC-CO₂ inactivation
231 of *B. diminuta* and *A. niger*. In general terms, the higher the pressure and the
232 temperature, the faster the inactivation. As an example, a reduction of only 4.4 log-cycles
233 of *A. niger* was achieved in 90 min at 100 bar and 50°C, while the complete inactivation
234 (6.7 log-cycles) was reached in just 15 min at 350 bar and 60°C (Fig. 1C). However, only

235 the temperature had a significant ($p < 0.05$) effect on the inactivation of *E. coli*. For
236 example, complete inactivation (7.9 log-cycles) was reached in 25 min at 35°C while the
237 same inactivation was achieved in less than 13 min at 50°C, regardless of the pressure
238 used (Fig. 1A). Moreover, when modelling the inactivation kinetics, less time was
239 generally required to achieve the complete inactivation of the *E. coli*, *B. diminuta* and
240 *A. niger* population ($t_{7.9}$, $t_{8.1}$ and $t_{6.8}$; respectively), as the pressure and the temperature
241 increased (Table 1). For example, in the case of *A. niger*, 163.7 and 22.1 min were
242 required at 100 bar and 50°C and at 350 bar and 60°C, respectively. On the one hand,
243 high temperatures are known to increase CO₂ diffusivity and make cell membranes more
244 fluid, facilitating the penetration of CO₂ [27,28]. On the other hand, high pressures
245 increase the solubility of CO₂ in the media [6]; therefore, there is closer contact between
246 CO₂ and the microbial cell, and the CO₂ penetration into the cells is improved [29,30].

247 Several authors also studied the SC-CO₂ inactivation of *E. coli* and *A. niger* in water
248 solutions [31–35]. However, only one study was found into the inactivation of *B. diminuta*
249 [21]. Norman et al. [31] also found that there was notably greater inactivation of *A. niger*
250 spores at higher pressures and temperatures (e.g. in 60 min and at a temperature of
251 55°C, microbial reduction increased from 2.8 log-cycles at 300 bar to 4.1 at 350 bar, and
252 at a constant pressure of 350 bar it increased from 2.0 to 4.6 log-cycles at temperatures
253 of 35 and 55°C, respectively). The inactivation levels achieved by Norman et al. [31] were
254 of a lower magnitude than those in the present study (e.g. 6.8 log-cycles was achieved
255 at 350 bar, 50°C and 55 min). As for *E. coli*, Dillow et al. [35] reported similar effects of
256 pressure and temperature to those in our study, since the temperature (34 vs 42°C)
257 affected the inactivation, achieving complete inactivation (around 8.0 log-cycles) in 30
258 min at 34°C and in 20 min at 42°C (205 bar), while the influence of pressure was
259 negligible (from 140 to 205 bar at 34°C). Ortuño et al. [12] also found very similar
260 reductions in the inactivation of *E. coli* in LB Broth, compared to the present results (e.g.
261 8.0 log-cycles were achieved at 36°C and 350 bar in 22 min, while in the present study
262 the same inactivation was found in 24 min at 35°C and 350 bar). However, these authors
263 found that both temperature (31-41 °C) and pressure (100-350 bar) influenced microbial
264 inactivation. As regards *B. diminuta*, Gomez-Gomez et al. [21] also found that the higher
265 the pressure and temperature, the higher the inactivation levels in an oil-in-water
266 emulsion. However, the processing time required to achieve the complete inactivation of
267 *B. diminuta* in the emulsions was longer than in the present study under the same
268 conditions (e.g. 40 min were required in the lipid emulsion while only 10 min in water
269 (Fig. 1B) at 350 bar and 50°C). This was coherent with what can be found in literature,
270 since SC-CO₂ inactivation treatments have proven to be more effective in simple media

271 than in complex and, in addition, oil is known to protect the microorganisms from different
272 external stresses, including SC-CO₂ [14,21].

273 Effect of the type of microorganism

274 As for the resistance of the different microorganisms studied to the SC-CO₂ treatments,
275 significant ($p < 0.05$) differences were found, *A. niger* being the most resistant of all three
276 microorganisms. On the contrary, very slight differences were found between *E. coli* and
277 *B. diminuta*. At 50°C and 350 bar, 55 min were required to achieve the complete
278 inactivation of *A. niger* (6.8 log-cycles), while around 10 min were needed for *E. coli* or
279 *B. diminuta* (around 8 log-cycles). This observation was coherent with the fact that fungal
280 spores are more resistant to SC-CO₂ treatments than vegetative bacteria [23], probably
281 due to their different and more resistant structure. Fungal spores are composed of a multi
282 layered and highly dehydrated structure, which could restrain the CO₂ dissolution and
283 penetration into the spore. Moreover, the structure of *A. niger* spores, in particular, include
284 a layer of melanin, which is believed to be related to a higher resistance to environmental
285 stresses [36]. Similarly, Wu et al. [37] achieved a reduction of 4.3 log-cycles for *E. coli* at
286 78 bar, 35°C and in 30 min, while only an inactivation of 2.1 log-cycles was obtained for
287 *Absidia coerulea* spores.

288 3.1.2. SC-CO₂ + HPU microbial inactivation

289 The combined SC-CO₂ + HPU inactivation kinetics of *E. coli* (A), *B. diminuta* (B) and
290 *A. niger* (C) are shown in Fig. 2. As in the SC-CO₂ kinetics (Fig. 1), the experimental
291 variability was high due to the aforementioned factors and the additional variability
292 related to the behaviour of the HPU transducer under supercritical conditions. The
293 Weibull model fitted the experimental data satisfactorily (Fig. 2), with a R² value higher
294 than 0.95 and a RMSE lower than 0.59 (Table 2). In addition, every n value in the
295 treatments with HPU (Table 2) was lower than 1 (from 0.26 to 0.56), which indicated that
296 the shape of every curve was concave upward.

297 Effect of pressure and temperature

298 The higher the pressure and temperature, the higher the level of inactivation of the SC-
299 CO₂ + HPU treatments for *B. diminuta* and *A. niger*. However, only the temperature had
300 a significant ($p < 0.05$) effect on the inactivation, as also occurred in the SC-CO₂
301 treatments. With respect to *E. coli* (Fig. 2A), in order to achieve complete inactivation
302 (7.9 log-cycles), raising the temperature from 35 to 50°C meant that 2.5 min (from 5.5 to
303 3 min) less were needed, on average; however, only 0.5 min (from 4.5 to 4 min) less
304 were needed when the pressure is raised from 100 to 350 bar. On the other hand, on

305 average, the time required to achieve the complete inactivation of *B. diminuta* (8.1 log-
306 cycles), was shortened from 12 to 6.5 min by raising the temperature from 35 to 50°C
307 and from 15 to 3.5 min when the pressure was increased from 100 to 350 bar (Fig. 2B).
308 The effect of the temperature was also revealed by the time needed for complete
309 inactivation (t_x) calculated by the Weibull model (Table 2). As an example, for *A. niger*,
310 $t_{6.8}$ was shortened on average from 63.4 min to 23.1 min when the temperature was
311 raised from 50 to 60°C. Contrary to the results of the present study, some authors found
312 that the increase in the pressure and temperature in the SC-CO₂ + HPU treatments did
313 not affect the microbial inactivation rate, probably because the marked effect of cavitation
314 masked the effects of the other processing conditions [12,17,38]. However, Gomez-
315 Gomez et al. [21] found that the higher the pressure and temperature, the higher the
316 level of SC-CO₂ + HPU inactivation for *E. coli* and *B. diminuta* in oil-in-water emulsions.

317 Effect of HPU and the type of microorganism

318 As in the SC-CO₂ treatments, significant ($p < 0.05$) differences were found as regards the
319 resistance of the different microorganisms to the combined SC-CO₂ + HPU treatment.
320 *A. niger* was the most resistant, while *E. coli* and *B. diminuta* showed similar resistance.
321 In fact, the complete inactivation of *E. coli* and *B. diminuta* was achieved in less than 18
322 min, even at low temperatures and pressures (100 bar and 35°C), whereas for *A. niger*,
323 at least 35 min were required to obtain complete inactivation at the same pressure (100
324 bar) and higher temperatures (50-60°C), which was considered too long a treatment for
325 industrial applications. The use of a higher pressure (350 bar) and 60°C was necessary
326 to achieve the complete inactivation of *A. niger* in a shorter time (10 min), which could
327 be considered a reasonable industrial processing time.

328 HPU significantly ($p < 0.05$) intensified the SC-CO₂ treatments for all the microorganisms
329 considered in the present study, the effect being milder in the case of *A. niger* spores
330 than for *E. coli* and *B. diminuta* (on average, the increase in the inactivation when HPU
331 was used was 1.3, 4.8 and 3.4 log-cycles, respectively). For instance, as observed in
332 Figs. 1 and 2, the time needed for the complete inactivation of *E. coli* and *B. diminuta* at
333 50°C and 350 bar was shortened by 19 min when HPU was applied; in the case of
334 *A. niger*, on the other hand, the process was shortened by only 5 min. Thus, the
335 application of HPU reduced the calculated t_x , on average; from 59.1 to 24.8 min (Tables
336 1 and 2). HPU is known to increase the mass and heat transfer under SC-CO₂ conditions
337 [39,40] and, consequently, to enhance both the CO₂ solubilisation in the media and
338 penetration inside the microbial cells [41]. Moreover, HPU could cause cracked or
339 damaged cell walls due to the effects of cavitation [38].

340 Several authors [12,38,42] also studied the application of HPU during the SC-CO₂
341 treatments of vegetative cells in liquid media and found that HPU drastically increased
342 the inactivation level.

343 The inactivation of different microorganisms depended not only on the effect of external
344 stresses, but also on the cell size and morphology [43,44]. Ortuño et al. [17] related the
345 degree of cavitation to the size of the vegetative cells since they observed a stronger
346 effect of cavitation on *S. cerevisiae* (8–10 µm) than on *E. coli* and assumed that there
347 was a greater likelihood of the cavitation bubbles affecting the cell structure when the
348 cells are larger. However, in the present study, there was probably not a big enough
349 difference between the sizes of the *E. coli* and *B. diminuta* cells (a difference of less than
350 2 µm) to appreciate significant differences in the SC-CO₂ + HPU inactivation between
351 these microorganisms, as also reported by Gomez-Gomez et al. [21]. In the case of
352 *A. niger* spores, the cell size (around 4 µm [45]) is larger than in *E. coli* and *B. diminuta*.
353 However, it is known that molds are generally more resistant to cavitation than vegetative
354 cells because of the differences between the cell wall structure of species [46]. In
355 particular, *A. niger* spores might be more resistant to cavitation due to the greater rigidity
356 of its cell wall due to the presence of melanin [36].

357

358 3.2. Analysis of the ultrastructure of microbial cells inactivated by SC-CO₂ + HPU

359 CryoFESEM and TEM images of the microbial cells after and before the SC-CO₂ + HPU
360 treatment are presented in Figs. 3 and 4, respectively.

361 The untreated *E. coli* cells showed an intact, well-defined and characteristic rod-shaped
362 structure with a smooth surface (Fig. 3A). The cell wall and the cell membrane presented
363 defined boundaries and were intact, enclosing the cytoplasmic content. In addition, the
364 cell wall can be seen to be attached to the cell membrane (Fig. 4A). As regards the
365 intracellular space, it is observed to be completely and uniformly filled with the cytoplasm
366 (Fig. 4A), with no signs of cytoplasm observed outside the cells. On the contrary, the
367 *E. coli* cells treated with SC-CO₂ + HPU lost their shape (Figs. 3B and 4B), appeared
368 agglomerated and some of them merged, losing their individuality (Fig.3B). The cell walls
369 and membranes were seen to be blurred (Fig. 4B), which indicated that they were partly
370 disintegrated. Inside the cell, empty regions were observed (Fig. 4B), which could be due
371 to a large amount of cytoplasmic content released by the effect of the treatment. This is
372 indicated by the stains being found in the extracellular region (Fig. 4B). Ortuño et al. [17]
373 observed important morphological changes in *E. coli* cells treated with SC-CO₂ + HPU
374 at 350 bar, 36°C for 5 min. The cytoplasmic space presented big empty regions with an

375 aggregated and unevenly distributed cytoplasm. In addition, the cell wall and membrane
376 appeared disintegrated. On the contrary, after a SC-CO₂ treatment under the same
377 conditions, *E. coli* cells only presented slight changes.

378 *B. diminuta* cells also presented a clear rod-shaped structure with a smooth surface
379 when untreated (Fig. 3C). The cell walls and membranes were intact and well-defined,
380 (Figs. 3C and 4C) enclosing the cytoplasm, which was uniformly distributed in the whole
381 intracellular space (Fig. 4C). Thus, the SC-CO₂ + HPU treatment caused different
382 alterations in the bacteria morphology. The surface appeared irregular with roughness
383 and wrinkles and some bacteria were found merged together (Fig. 3D). The cell walls
384 and membranes were undefined (Fig. 4D), indicating that they were damaged. In
385 addition, empty regions in the intracellular space were observed (Fig. 4D), indicating that
386 a great amount of cytoplasmic content was lost with the treatment. No studies were found
387 analyzing the ultrastructure of *B. diminuta* cells treated with either SC-CO₂ or SC-CO₂ +
388 HPU.

389 *B. diminuta* and *E. coli* cells were both similarly affected by the SC-CO₂ + HPU treatment.
390 As several authors [15,17,47] observed in the case of SC-CO₂ treatments, the
391 morphological structure of the microbial cells, including the cell wall, generally remained
392 almost intact or with only minor alterations, while changes in the intracellular structure,
393 such as an uneven distribution of the cytoplasm, were found. Consequently, it could be
394 stated that the inactivation effect was probably due to an increase in the permeability of
395 the cells exerted by SC-CO₂, instead of to the rupture of the cell wall and membrane. By
396 contrast, the application of HPU could crack or damage cell walls, severely affecting their
397 morphological integrity [17], as observed in the images of the present study (Figs.3 and
398 4).

399 In the case of *A. niger* spores, untreated cells presented a globular shape and a spiny,
400 wrinkled surface (Fig. 3E). The cell wall and membrane showed defined boundaries and
401 uniform thickness (Fig.4E). In addition, in the intracellular region, the organelles were
402 clearly visible and well distributed in a dense cytoplasm (Fig.4E). In contrast, *A. niger*
403 spores treated with SC-CO₂ + HPU demonstrated significant alterations. The shape of
404 the cell changed, since it appeared shrunken and squashed and most of the cells
405 presented a clear cleft in the center (Figs. 3F and 4F). After the treatment, the cell wall
406 appeared much thinner than that of the untreated spores, showing an uneven width with
407 some dissolved areas (Fig. 4F). Moreover, the cell membrane was also thinner and
408 presented an uneven thickness (Fig. 4F). As to the inner region of the spore, it was
409 almost empty due to leakages of cytoplasmic content (Fig. 4F) and the organelles were
410 not visible, indicating that they were completely destroyed after the treatment. Only a
411 small, darker region was found in the cytoplasm, which could be due to the precipitation

412 or aggregation of internal cell components (Fig. 4F). Although no studies were found
413 assessing the ultrastructural changes in *A. niger* spores after SC-CO₂ + HPU treatments,
414 Noman et al. [31] and Efaq et al. [48] observed the morphology of *A. niger* spores treated
415 with SC-CO₂ at 300 bar, 75 °C for 90 min. These authors found completely damaged
416 and deformed spores, with disintegrated cell wall and membrane. Nevertheless, an
417 extremely long process time was used in those studies (90 min) and a higher
418 temperature than in the present study (75°C vs 60°C).

419 In general terms, an ultrastructural analysis revealed that for the three microorganisms
420 involved in the present study, the combined SC-CO₂ + HPU treatment damaged the cell
421 walls and affected the permeability of cell membranes, which led to changes in the cell
422 morphology and the release of cytoplasmic content and, consequently, cell death.

423

424 **4. Conclusions**

425 Ultrasonic application has proven to be an effective way of shortening the inactivation
426 time in SC-CO₂ treatments of the microorganisms studied (two vegetative bacteria and
427 one fungal spore). The higher the pressure and the temperature, the greater the
428 inactivation of *B. diminuta* and *A. niger*. However, it was only the temperature that had a
429 significant effect on *E.coli*. The results obtained confirmed the more marked effect that
430 cavitation has on the SC-CO₂ inactivation of vegetative bacteria, compared to fungal
431 spores.

432 The ultrastructural analysis illustrated the external morphology and intracellular structure
433 of bacteria (*E. coli* and *B. diminuta*) and fungal spores (*A. niger*), which definitively
434 contributed to a better understanding of the effects of the SC-CO₂ + HPU treatments.
435 SC-CO₂ + HPU-treated cells presented a deformed shape, partly disintegrated walls and
436 membranes and a leakage of cytoplasmic content, which explains the effectiveness of
437 the SC-CO₂ + HPU treatments for microbial inactivation purposes. Thus, regardless of
438 the type of microorganism (vegetative bacteria or fungal spore) and its different cell wall
439 structure and composition, the SC-CO₂ + HPU treatment caused structural damage
440 leading to cell death. Further research into the ultrastructure of other fungal or bacterial
441 spores in different complex media is required to elucidate the exact inactivation
442 mechanisms of the SC-CO₂ + HPU technology.

443

444 **Acknowledgement**

445 The authors acknowledge the financial support from Fresenius Kabi.

446

447 **References**

- 448 [1] H.M. Lung, Y.C. Cheng, Y.H. Chang, H.-W. Huang, B.B. Yang, C.Y. Wang,
449 Microbial decontamination of food by electron beam irradiation, *Trends Food Sci.*
450 *Technol.* 44 (2015) 66–78. <https://doi.org/10.1016/j.tifs.2015.03.005>.
- 451 [2] D. Knorr, M. Zenker, V. Heinz, D.U. Lee, Applications and potential of ultrasonics
452 in food processing, *Trends Food Sci. Technol.* 15 (2004) 261–266.
453 <https://doi.org/10.1016/j.tifs.2003.12.001>.
- 454 [3] S. Spilimbergo, F. Dehghani, A. Bertucco, N.R. Foster, Inactivation of bacteria
455 and spores by pulse electric field and high pressure CO₂ at low temperature,
456 *Biotechnol. Bioeng.* 82 (2003) 118–125. <https://doi.org/10.1002/bit.10554>.
- 457 [4] C. Ortuño, T. Duong, M. Balaban, J. Benedito, Combined high hydrostatic
458 pressure and carbon dioxide inactivation of pectin methylesterase, polyphenol
459 oxidase and peroxidase in feijoa puree, *J. Supercrit. Fluids.* 82 (2013) 56–62.
460 <https://doi.org/10.1016/j.supflu.2013.06.005>.
- 461 [5] C. Ortuño, M.T. Martínez-Pastor, A. Mulet, J. Benedito, Supercritical carbon
462 dioxide inactivation of *Escherichia coli* and *Saccharomyces cerevisiae* in
463 different growth stages, *J. Supercrit. Fluids.* 63 (2012) 8–15.
464 <https://doi.org/10.1016/J.SUPFLU.2011.12.022>.
- 465 [6] S. Damar, M.O. Balaban, Review of dense phase CO₂ technology: microbial
466 and enzyme inactivation, and effects on food quality, *J. Food Sci.* 71 (2006) 1–
467 11.
- 468 [7] G. Ferrentino, M.L. Plaza, M. Ramirez-Rodrigues, G. Ferrari, M.O. Balaban,
469 Effects of dense phase carbon dioxide pasteurization on the physical and quality
470 attributes of a red grapefruit juice, *J. Food Sci.* 74 (2009).
471 <https://doi.org/10.1111/j.1750-3841.2009.01250.x>.
- 472 [8] F. Gasperi, E. Aprea, F. Biasioli, S. Carlin, I. Endrizzi, G. Pirretti, S. Spilimbergo,
473 Effects of supercritical CO₂ and N₂O pasteurisation on the quality of fresh apple
474 juice, *Food Chem.* 115 (2009) 129–136.
475 <https://doi.org/10.1016/j.foodchem.2008.11.078>.
- 476 [9] H. Liao, Y. Zhang, X. Hu, X. Liao, J. Wu, Behavior of inactivation kinetics of
477 *Escherichia coli* by dense phase carbon dioxide, *Int. J. Food Microbiol.* 126
478 (2008) 93–97. <https://doi.org/10.1016/J.IJFOODMICRO.2008.05.008>.
- 479 [10] G. Pataro, G. Ferrentino, C. Ricciardi, G. Ferrari, Pulsed electric fields assisted

- 480 microbial inactivation of *S. cerevisiae* cells by high pressure carbon dioxide, *J.*
481 *Supercrit. Fluids.* 54 (2010) 120–128.
482 <https://doi.org/10.1016/j.supflu.2010.04.003>.
- 483 [11] E. Shieh, A. Paszczynski, C.M. Wai, Q. Lang, R.L. Crawford, Sterilization of
484 *Bacillus pumilus* spores using supercritical fluid carbon dioxide containing
485 various modifier solutions, *J. Microbiol. Methods.* 76 (2009) 247–252.
486 <https://doi.org/10.1016/j.mimet.2008.11.005>.
- 487 [12] C. Ortuño, M.T. Martínez-Pastor, A. Mulet, J. Benedito, An ultrasound-enhanced
488 system for microbial inactivation using supercritical carbon dioxide, *Innov. Food*
489 *Sci. Emerg. Technol.* 15 (2012) 31–37.
490 <https://doi.org/10.1016/J.IFSET.2012.02.006>.
- 491 [13] G. Ferrentino, S. Spilimbergo, A combined high pressure carbon dioxide and
492 high power ultrasound treatment for the microbial stabilization of cooked ham, *J.*
493 *Food Eng.* 174 (2016) 47–55.
494 <https://doi.org/10.1016/J.JFOODENG.2015.11.013>.
- 495 [14] L. Garcia-Gonzalez, A.H. Geeraerd, K. Elst, L. Van Ginneken, J.F. Van Impe, F.
496 Devlieghere, Influence of type of microorganism, food ingredients and food
497 properties on high-pressure carbon dioxide inactivation of microorganisms, *Int. J.*
498 *Food Microbiol.* 129 (2009) 253–263.
499 <https://doi.org/10.1016/j.ijfoodmicro.2008.12.005>.
- 500 [15] L. Garcia-Gonzalez, A.H. Geeraerd, J. Mast, Y. Briers, K. Elst, L. Van Ginneken,
501 J.F. Van Impe, F. Devlieghere, Membrane permeabilization and cellular death of
502 *Escherichia coli*, *Listeria monocytogenes* and *Saccharomyces cerevisiae* as
503 induced by high pressure carbon dioxide treatment, *Food Microbiol.* 27 (2010)
504 541–549. <https://doi.org/10.1016/j.fm.2009.12.004>.
- 505 [16] H. Liao, F. Zhang, X. Liao, X. Hu, Y. Chen, L. Deng, Analysis of *Escherichia coli*
506 cell damage induced by HPCD using microscopies and fluorescent staining, *Int.*
507 *J. Food Microbiol.* 144 (2010) 169–176.
508 <https://doi.org/10.1016/j.ijfoodmicro.2010.09.017>.
- 509 [17] C. Ortuño, A. Quiles, J. Benedito, Inactivation kinetics and cell morphology of *E.*
510 *coli* and *S. cerevisiae* treated with ultrasound-assisted supercritical CO₂, *Food*
511 *Res. Int.* 62 (2014) 955–964. <https://doi.org/10.1016/J.FOODRES.2014.05.012>.
- 512 [18] G. Reshes, S. Vanounou, I. Fishov, M. Feingold, Cell shape dynamics in

- 513 Escherichia coli, *Biophys. J.* 94 (2008) 251–264.
514 <https://doi.org/10.1529/BIOPHYSJ.107.104398>.
- 515 [19] S. Sundaram, J. Eisenhuth, G. Howard, H. Brandwein, Retention of Water-Borne
516 Bacteria by Membrane Filters Part I: Bacterial Challenge Tests on 0.2 and 0.22
517 Micron Rated Filters, *PDA J. Pharm. Sci. Technol.* 55 (2001) 65–86.
- 518 [20] S.S. Madaeni, The application of membrane technology for water disinfection,
519 *Water Res.* 33 (1999) 301–308. [https://doi.org/10.1016/S0043-1354\(98\)00212-7](https://doi.org/10.1016/S0043-1354(98)00212-7).
- 520 [21] A. Gomez-Gomez, E. Brito-de la Fuente, C. Gallegos, J.V. Garcia-Perez, J.
521 Benedito, Non-thermal pasteurization of lipid emulsions by combined
522 supercritical carbon dioxide and high-power ultrasound treatment, *Ultrason.*
523 *Sonochem.* 67 (2020) 105–138.
524 <https://doi.org/10.1016/J.ULTSONCH.2020.105138>.
- 525 [22] M. Shimoda, H. Kago, N. Kojima, M. Miyake, Osajima, I. Hayakawa, Accelerated
526 death kinetics of *Aspergillus niger* spores under high-pressure carbonation, *Appl.*
527 *Environ. Microbiol.* 68 (2002) 4162–4167.
528 <https://doi.org/10.1128/AEM.68.8.4162>.
- 529 [23] G.C. Soares, D.A. Learmonth, M.C. Vallejo, S.P. Davila, P. González, R.A.
530 Sousa, A.L. Oliveira, Supercritical CO₂ technology: The next standard
531 sterilization technique?, *Mater. Sci. Eng. C.* 99 (2019) 520–540.
532 <https://doi.org/10.1016/J.MSEC.2019.01.121>.
- 533 [24] M. Peleg, On calculating sterility in thermal and non-thermal preservation
534 methods, *Food Res. Int.* 32 (1999) 271–278. [https://doi.org/10.1016/S0963-](https://doi.org/10.1016/S0963-9969(99)00081-2)
535 [9969\(99\)00081-2](https://doi.org/10.1016/S0963-9969(99)00081-2).
- 536 [25] M. Peleg, *Models for predicting growth and inactivation. Advanced quantitative*
537 *microbiology for foods and biosystems*, 2006.
- 538 [26] A. Gomez-Gomez, E. Brito-de la Fuente, C. Gallegos, J.V. Garcia-Perez, J.
539 Benedito, Ultrasonic-assisted supercritical CO₂ inactivation of bacterial spores
540 and effect on the physicochemical properties of oil-in-water emulsions, *J.*
541 *Supercrit. Fluids.* 174 (2021) 105246.
542 <https://doi.org/10.1016/j.supflu.2021.105246>.
- 543 [27] S.I. Hong, W.S. Park, Y.R. Pyun, Non-thermal inactivation of *Lactobacillus*
544 *plantarum* as influenced by pressure and temperature of pressurized carbon
545 dioxide, *Int. J. Food Sci. Technol.* 34 (1999) 125–130.

- 546 <https://doi.org/10.1046/j.1365-2621.1999.00241.x>.
- 547 [28] G. Ferrentino, S. Spilimbergo, High pressure carbon dioxide combined with high
548 power ultrasound pasteurization of fresh cut carrot, *J. Supercrit. Fluids.* 105
549 (2015) 170–178. <https://doi.org/10.1016/J.SUPFLU.2014.12.014>.
- 550 [29] H. Liao, X. Hu, X. Liao, F. Chen, J. Wu, Inactivation of *Escherichia coli*
551 inoculated into cloudy apple juice exposed to dense phase carbon dioxide, *Int. J.*
552 *Food Microbiol.* 118 (2007) 126–131.
553 <https://doi.org/10.1016/J.IJFOODMICRO.2007.06.018>.
- 554 [30] S.I. Hong, W.S. Park, Y.R. Pyun, Inactivation of *Lactobacillus* sp. from Kimchi by
555 high pressure carbon dioxide, *LWT - Food Sci. Technol.* 30 (1997) 681–685.
556 <https://doi.org/10.1006/FSTL.1997.0250>.
- 557 [31] E. Noman, N. Norulaini Nik Ab Rahman, A. Al-Gheethi, H. Nagao, B.A. Talip, O.
558 Ab. Kadir, Selection of inactivation medium for fungal spores in clinical wastes
559 by supercritical carbon dioxide, *Environ. Sci. Pollut. Res.* 25 (2018) 21682–
560 21692. <https://doi.org/10.1007/s11356-018-2335-1>.
- 561 [32] P. Ballestra, J.L. Cuq, Influence of pressurized carbon dioxide on the thermal
562 inactivation of bacterial and fungal spores, *LWT - Food Sci. Technol.* 31 (1998)
563 84–88. <https://doi.org/10.1006/fstl.1997.0299>.
- 564 [33] H.G. Yuk, D.J. Geveke, H.Q. Zhang, Non-thermal inactivation of *Escherichia coli*
565 K12 in buffered peptone water using a pilot-plant scale supercritical carbon
566 dioxide system with a gas-liquid porous metal contactor, *Food Control.* 20 (2009)
567 847–851. <https://doi.org/10.1016/j.foodcont.2008.10.004>.
- 568 [34] F. Kobayashi, Y. Hayata, K. Kohara, N. Muto, Y. Osajima, Application of
569 supercritical CO₂ bubbling to inactivate *E. coli* and coliform bacteria in drinking
570 water, *Food Sci. Technol. Res.* 13 (2007) 20–22.
571 <https://doi.org/10.3136/fstr.13.20>.
- 572 [35] A.K. Dillow, F. Dehghani, J.S. Hrkach, N.R. Foster, R. Langer, Bacterial
573 inactivation by using near- and supercritical carbon dioxide, *Proc. Natl. Acad.*
574 *Sci. U. S. A.* 96 (1999) 10344–10348. <https://doi.org/10.1073/pnas.96.18.10344>.
- 575 [36] B.Y. Tischler, T.M. Hohl, Menacing mold: recent advances in *Aspergillus*
576 pathogenesis and host defense, *J. Mol. Biol.* 431 (2019) 4229–4246.
577 <https://doi.org/10.1016/j.jmb.2019.03.027>.
- 578 [37] Y. Wu, S.J. Yao, Y.X. Guan, Inactivation of microorganisms in carbon dioxide at

- 579 elevated pressure and ambient temperature, *Ind. Eng. Chem. Res.* 46 (2007)
580 6345–6352. <https://doi.org/10.1021/ie0702330>.
- 581 [38] C. Ortuño, M.T. Martínez-Pastor, A. Mulet, J. Benedito, Application of high
582 power ultrasound in the supercritical carbon dioxide inactivation of
583 *Saccharomyces cerevisiae*, *Food Res. Int.* 51 (2013) 474–481.
584 <https://doi.org/10.1016/J.FOODRES.2013.01.041>.
- 585 [39] Y. Gao, B. Nagy, X. Liu, B. Simándi, Q. Wang, Supercritical CO₂ extraction of
586 lutein esters from marigold (*Tagetes erecta* L.) enhanced by ultrasound, *J.*
587 *Supercrit. Fluids.* 49 (2009) 345–350.
588 <https://doi.org/10.1016/J.SUPFLU.2009.02.006>.
- 589 [40] J.A. Cárcel, J.V. García-Pérez, J. Benedito, A. Mulet, Food process innovation
590 through new technologies: Use of ultrasound, *J. Food Eng.* 110 (2012) 200–207.
591 <https://doi.org/10.1016/J.JFOODENG.2011.05.038>.
- 592 [41] L. Garcia-Gonzalez, A.H. Geeraerd, S. Spilimbergo, K. Elst, L. Van Ginneken, J.
593 Debevere, J.F. Van Impe, F. Devlieghere, High pressure carbon dioxide
594 inactivation of microorganisms in foods: The past, the present and the future, *Int.*
595 *J. Food Microbiol.* 117 (2007) 1–28.
596 <https://doi.org/10.1016/j.ijfoodmicro.2007.02.018>.
- 597 [42] I. Paniagua-Martínez, A. Mulet, M.A. García-Alvarado, J. Benedito, Ultrasound-
598 assisted supercritical CO₂ treatment in continuous regime: Application in
599 *Saccharomyces cerevisiae* inactivation, *J. Food Eng.* 181 (2016) 42–49.
600 <https://doi.org/10.1016/J.JFOODENG.2016.02.024>.
- 601 [43] B. Tonyali, A. McDaniel, V. Trinetta, U. Yucel, Evaluation of heating effects on
602 the morphology and membrane structure of *Escherichia coli* using electron
603 paramagnetic resonance spectroscopy, *Biophys. Chem.* 252 (2019) 106191.
604 <https://doi.org/10.1016/J.BPC.2019.106191>.
- 605 [44] F. Chemat, Zill-E-Huma, M.K. Khan, Applications of ultrasound in food
606 technology: Processing, preservation and extraction, *Ultrason. Sonochem.* 18
607 (2011) 813–835. <https://doi.org/10.1016/j.ultsonch.2010.11.023>.
- 608 [45] W.R. Teertstra, M. Tegelaar, J. Dijksterhuis, E.A. Golovina, R.A. Ohm, H.A.B.
609 Wösten, Maturation of conidia on conidiophores of *Aspergillus niger*, *Fungal*
610 *Genet. Biol.* 98 (2017) 61–70. <https://doi.org/10.1016/j.fgb.2016.12.005>.
- 611 [46] A. López-Malo, E. Palou, M. Jiménez-Fernández, S.M. Alzamora, S. Guerrero,

- 612 Multifactorial fungal inactivation combining thermosonication and antimicrobials,
613 J. Food Eng. 67 (2005) 87–93. <https://doi.org/10.1016/j.jfoodeng.2004.05.072>.
- 614 [47] S. Spilimbergo, D. Mantoan, A. Dalser, Supercritical gases pasteurization of
615 apple juice, J. Supercrit. Fluids. 40 (2007) 485–489.
616 <https://doi.org/10.1016/J.SUPFLU.2006.07.013>.
- 617 [48] A.N. Efaq, N.N.N. Nik Norulaini, H. Nagao, A.A. Al-Gheethi, M.O. Ab. Kadir,
618 Inactivation of Aspergillus spores in clinical wastes by supercritical carbon
619 dioxide, Arab. J. Sci. Eng. 42 (2017) 39–51. [https://doi.org/10.1007/s13369-016-](https://doi.org/10.1007/s13369-016-2087-5)
620 [2087-5](https://doi.org/10.1007/s13369-016-2087-5).
- 621

- HPU increased the SC-CO₂ inactivation of *E. coli*, *B. diminuta* and *A. niger*.
- The higher the pressure and temperature, the greater the SC-CO₂+HPU inactivation.
- *A. niger* spores were found to be more resistant than vegetative bacteria.
- Microscopy analysis revealed significant morphological changes to the microbial cells.
- SC-CO₂ + HPU inactivation was effective for all the microorganisms despite their cell structure.

Fig. 1. Inactivation kinetics of *E. coli* (A), *B. diminuta* (B) and *A. niger* spores (C) in water treated with SC-CO₂. Experimental data (discrete points) and Weibull model (continuous and dashed lines). Error bars show the experimental variability.

Fig. 2. Inactivation kinetics of *E. coli* (A), *B. diminuta* (B) and *A. niger* spores (C) in water treated with SC-CO₂ + HPU. Experimental data (discrete points) and Weibull model (continuous and dashed lines). Error bars show the experimental variability.

Fig. 3. CryoFESEM photographs of *E. coli* (A and B), *B. diminuta* (C and D) and *A. niger* (E and F) untreated and treated by SC-CO₂ + HPU.

Fig. 4. TEM photographs of *E. coli* (A and B), *B. diminuta* (C and D) and *A. niger* (E and F) untreated and treated by SC-CO₂ + HPU.

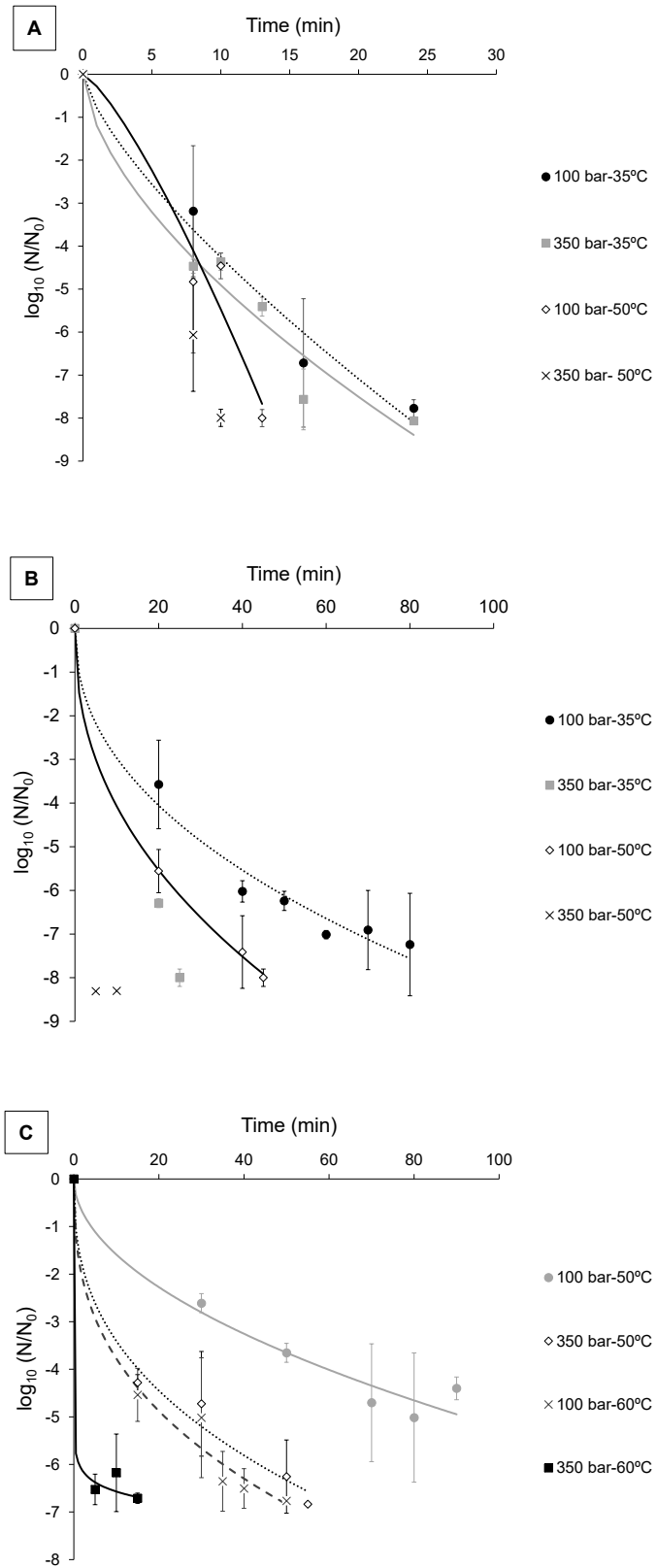


Fig. 1.

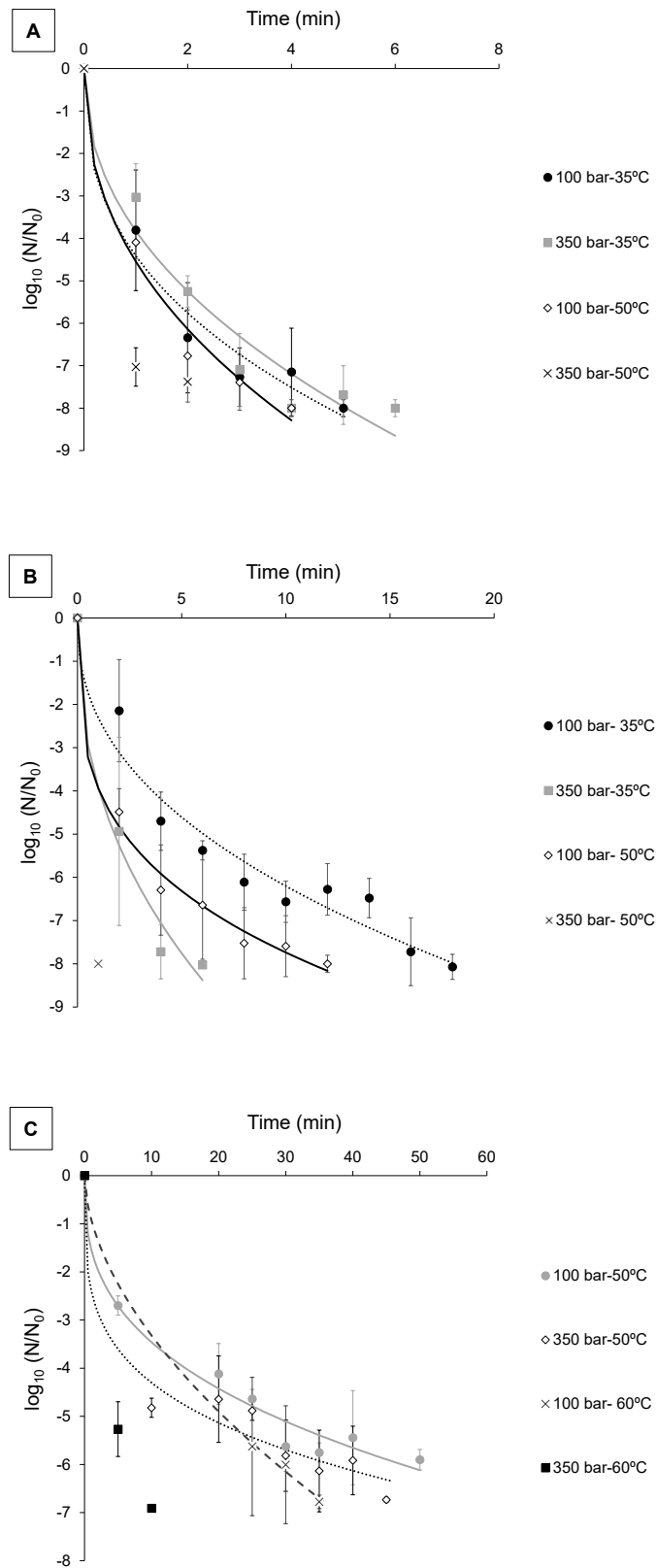


Fig. 2.

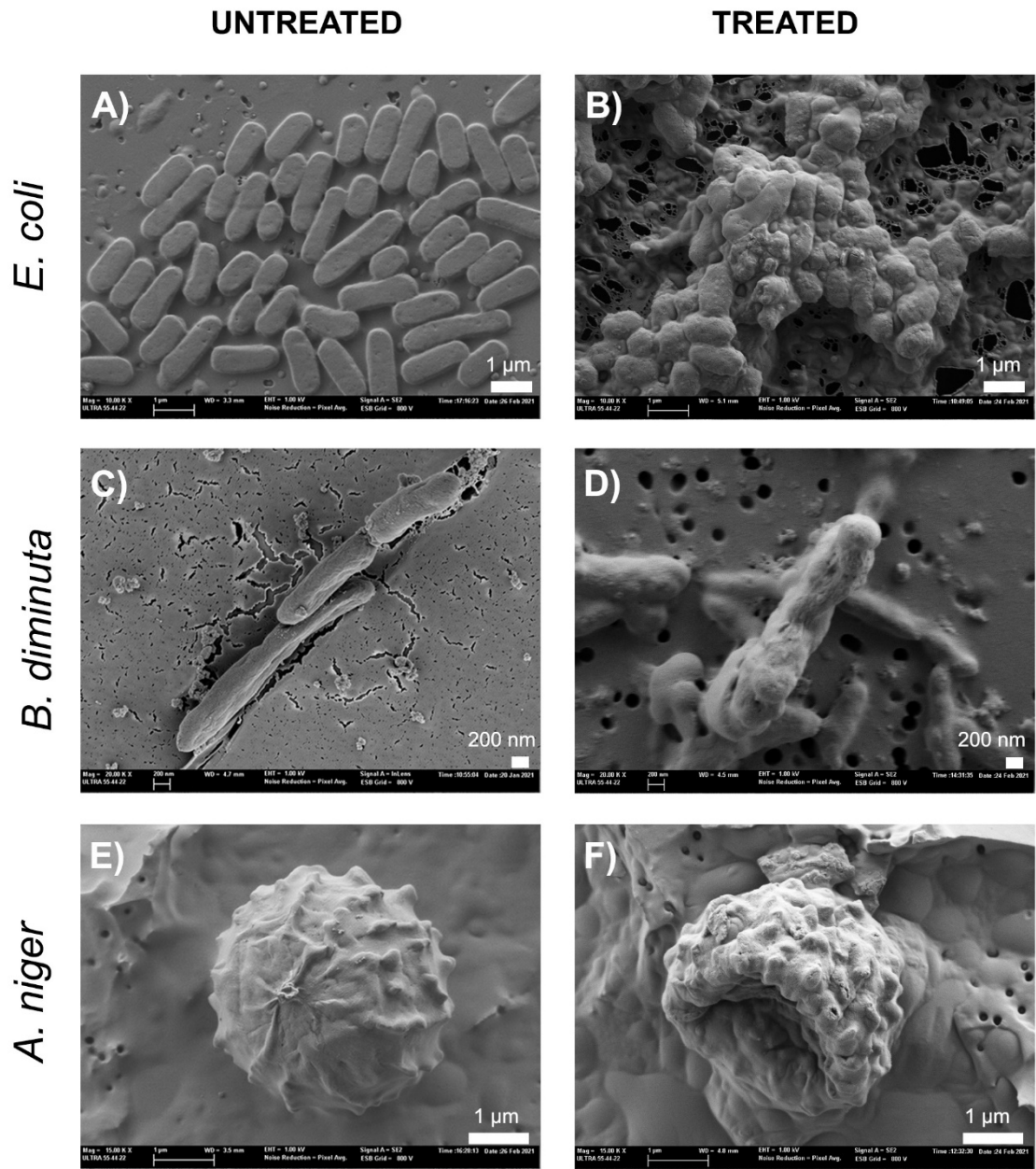


Fig. 3.

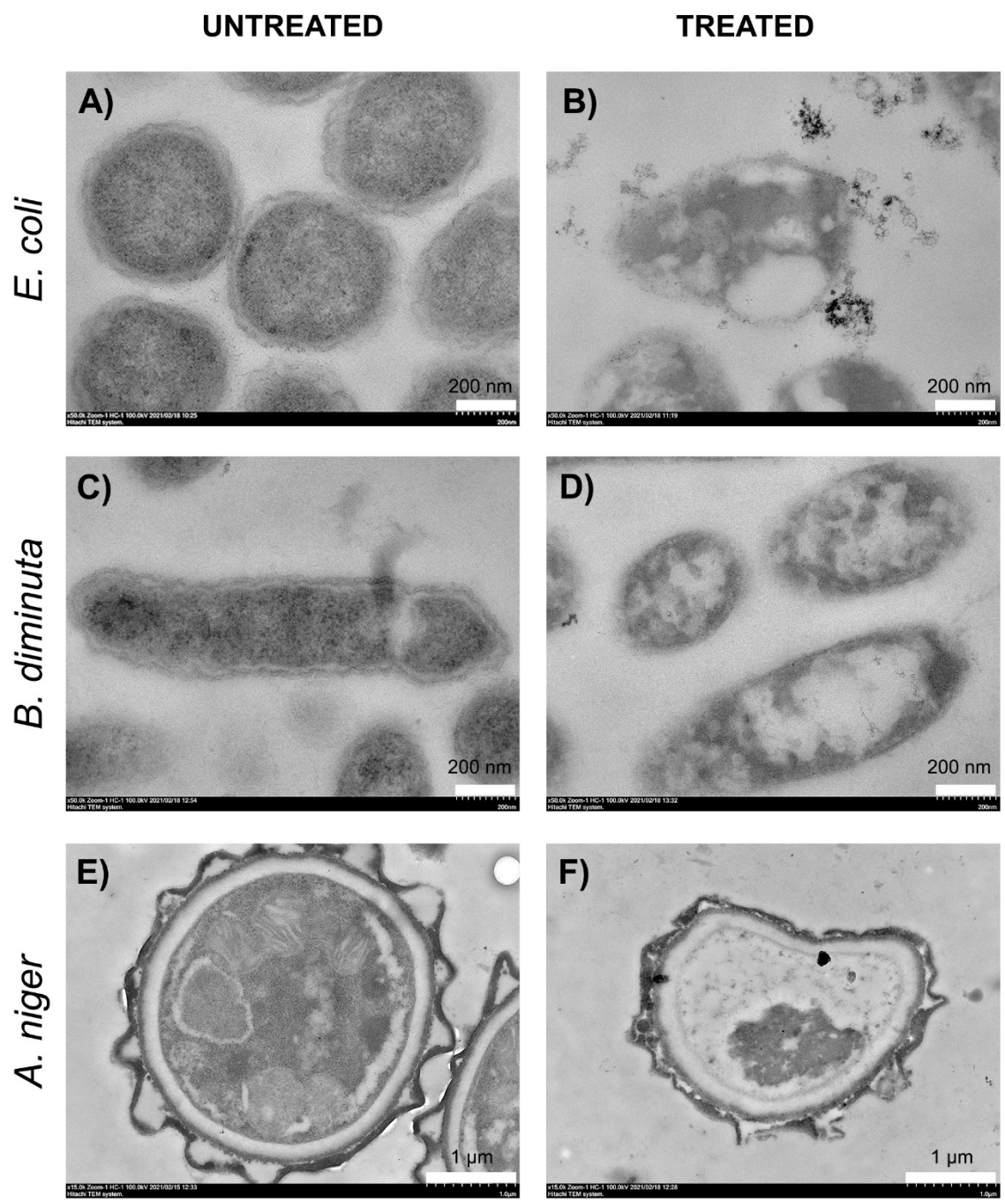


Fig. 4.

Table 1. Fitting of Weibull model to SC-CO₂ inactivation kinetics in distilled water. Parameters (b and n), total time for complete inactivation of *E. coli* (t_{7.9}; 7.9 log-cycle reduction) , *B. diminuta* (t_{8.1}; 8.1 log-cycle reduction) and *A. niger* (t_{6.8}; 6.8 log-cycle reduction) and statistical parameters (R² and RMSE). Average values and standard errors (in brackets).

Microorganism	Pressure (bar)	Temperature (°C)	b (min ⁻ⁿ)	n	t _{7.9/8.1/6.8} (min)	R ²	RMSE
<i>E. coli</i>	100	35	0.84 (0.38)	0.72 (0.16)	22.5	0.97	0.46
<i>E. coli</i>	350	35	1.20 (0.40)	0.61 (0.12)	22.0	0.95	0.52
<i>E. coli</i>	100	50	0.28 (0.33)	1.29 (0.48)	13.3	0.92	0.64
<i>E. coli</i>	350	50	*	*	*	*	*
<i>B. diminuta</i>	100	35	1.06 (0.30)	0.45 (0.07)	91.8	0.98	0.33
<i>B. diminuta</i>	350	35	*	*	*	*	*
<i>B. diminuta</i>	100	50	1.48 (0.13)	0.44 (0.03)	47.6	0.99	0.07
<i>B. diminuta</i>	350	50	*	*	*	*	*
<i>A. niger</i>	100	50	0.48 (0.26)	0.52 (0.13)	163.7	0.96	0.31
<i>A. niger</i>	350	50	1.40 (1.50)	0.38 (0.27)	64.0	0.98	0.28
<i>A. niger</i>	100	60	1.62 (0.48)	0.37 (0.08)	48.3	0.98	0.32
<i>A. niger</i>	350	60	5.95 (0.40)	0.04 (0.02)	22.1	0.99	0.12

* Insufficient experimental data for model fitting

Table 2. Fitting of Weibull model to SC-CO₂ + HPU inactivation kinetics in distilled water. Parameters (b and n), total time for complete inactivation of *E. coli* (t_{7.9}; 7.9 log-cycle reduction) , *B. diminuta* (t_{8.1}; 8.1 log-cycle reduction) and *A. niger* (t_{6.8}; 6.8 log-cycle reduction) and statistical parameters (R² and RMSE). Average values and standard errors (in brackets).

Microorganism	Pressure (bar)	Temperature (°C)	b (min ⁻ⁿ)	n	t _{7.9/8.1/6.8} (min)	R ²	RMSE
<i>E. coli</i>	100	35	4.42 (0.43)	0.38 (0.08)	4.6	0.97	0.44
<i>E. coli</i>	350	35	3.82 (0.49)	0.46 (0.09)	4.9	0.95	0.59
<i>E. coli</i>	100	50	4.55 (0.40)	0.43 (0.08)	3.6	0.98	0.37
<i>E. coli</i>	350	50	*	*	*	*	*
<i>B. diminuta</i>	100	35	2.31 (0.34)	0.43 (0.06)	18.5	0.95	0.49
<i>B. diminuta</i>	350	35	3.93 (0.69)	0.42 (0.12)	8.0	0.98	0.41
<i>B. diminuta</i>	100	50	3.94 (0.26)	0.29 (0.03)	12.0	0.99	0.23
<i>B. diminuta</i>	350	50	*	*	*	*	*
<i>A. niger</i>	100	50	1.53 (0.27)	0.35 (0.05)	70.9	0.98	0.28
<i>A. niger</i>	350	50	2.39 (0.56)	0.26 (0.07)	55.8	0.96	0.37
<i>A. niger</i>	100	60	0.91 (0.50)	0.56 (0.16)	36.3	0.99	0.09
<i>A. niger</i>	350	60	*	*	*	*	*

* Insufficient experimental data for model fitting